Microfluid Nanofluid
DOI 10.1007/s10404-010-0650-z

RESEARCH PAPER

Solute dispersion in oscillating electro-osmotic flow with boundary mass exchange

Guy Ramon · Yehuda Agnon · Carlos Dosoretz

Received: 16 February 2010 / Accepted: 15 April 2010

Abstract Mass transfer in an oscillatory electro-osmotic flow (EOF) is theoretically studied, for the case of a cylindrical tube with a reactive wall. An expression for the dispersion coefficient, reflecting the time-averaged mass flux of an electrically neutral solute, is derived analytically. Under the influence of a reversible solute-wall mass exchange, the dispersion coefficient exhibits a complex dependence on the various parameters representing the effects of the electric double-layer thickness, oscillation frequency, solution transport properties, solute partitioning, and reaction kinetics. Our results suggest that, in the presence of a reversible mass exchange at the wall, an oscillatory EOF may be used for separation of species. It is found that optimal conditions for separation are achieved for a thin double-layer, where an inert solute, or one with slow exchange kinetics, experiences virtually no dispersion while the dispersion is maximized for the reactive solute exhibiting fast kinetics.

Keywords Oscillatory electro-osmotic flow · Taylor–Aris dispersion · Enhanced mass transfer · Solute separation

1 Introduction

Electro-osmotic flow (EOF) may be described as the bulk fluid motion, induced by an applied electric potential acting on excess ionic charges in an electrolyte solution. Such excess charges may be present due to the formation of an electric double layer (EDL) at the interface between the solution and a charged solid boundary (Probstein 2003). At the charged surface, co-ions are repelled while counter-ions are attracted; a diffuse layer is thus established, extending from the charged surface outward to the bulk, electro-neutral, solution. An externally applied electric field induces the migration of the ions within the EDL, which in turn results in the flow of the adjacent fluid by virtue of viscous momentum transfer.

Recent interest in micro- and nano-fluidic devices has seen a dramatic increase of studies directed at the analysis of EOF and associated transport phenomena, applied as a means of controlling fluid transport, mixing and/or separation (Stone et al. 2004; Chang and Yang 2007; Squires and Quake 2005). EOF, compared with pressure-driven flow, offers the ability to control and drive the fluid by external means and with no moving parts, allowing for miniaturization while maintaining high reliability and simplicity. An area of particularly intensive research has been the use of time-periodic EOF, which has been shown to enhance mixing in the generally diffusion-limited conditions prevailing at such small scales. The enhanced mixing achieved has been largely attributed to chaotic advection and electrokinetic instability (Chang and Yang 2007). The promise of such applications has also generated interest in the basic characteristics of EOF driven by alternating currents (AC-driven EOF). Analytical studies of AC-driven EOF in parallel-plate and cylindrical geometries have been performed by Kang et al. (2002), Yang et al. (2002), Bhattacharya et al. (2003) as well as by Dutta and Beskok (2001), who also compared the AC-driven EOF with the Stokes second problem of a boundary-driven oscillatory flow. Erickson and Li (2003) presented a comparison between a numerical and approximate analytical

G. Ramon (✉) · Y. Agnon · C. Dosoretz
Department of Civil and Environmental Engineering, Technion-Israel Institute of Technology, Haifa 32000, Israel
e-mail: ramong@tx.technion.ac.il

Published online: 16 June 2010

solution of the Poisson–Boltzmann and Navier–Stokes equations, governing the EOF driven by a time-periodic electric field with various waveforms. Their results illustrated that the analytical solution, based on the Debye–Hückel approximation, provides an adequate description of the induced velocity field.

Mass transfer in pressure-driven oscillatory flows has been studied extensively, since the pioneering work of Aris (1960) who calculated the dispersion coefficient of a passive solute using the method of moments. The basic mechanism for this type of dispersion is molecular diffusion occurring down lateral concentration gradients created by a non-uniform velocity field. This phenomenon is known as 'Taylor–Aris' dispersion, and results in the 'stretching' of a solute cloud in a viscous flow. This mechanism also exists in oscillating viscous flows; however, under appropriate conditions it may be possible to substantially increase the mass transfer of the solute (Joshi et al. 1983; Kurzweg et al. 1984), even though there is no net transfer of the carrier fluid. This time-averaged mass transfer may be described as the interplay between the bulk advection, which is highest in the regions far from the solid wall, and diffusion into and out of the wall region, where the fluid motion is retarded by viscosity. Thus, during an oscillation cycle, the solute first diffuses towards the slower moving regions of the cross-section, where it is temporarily 'stored'; it then diffuses back into the bulk flow and, in the presence of an axial concentration gradient and proper phasing between the oscillating velocity and concentration fields, is 'shuttled' along the axial direction.

Since this mode of mass transfer relies first and foremost upon the temporal 'storage' of material within a viscous boundary layer, it follows that other means of such 'storage' may yield a time-average mass flux as well. In the presence of a reversible reaction or phase exchange between the wall and the fluid, such a rectified motion of the solute may be possible, regardless of the velocity distribution. Dispersion in oscillating flows with a reversible, kinetic exchange with the solid boundary was studied by Ng (2006), who employed the method of homogenization to obtain an effective transport equation. It was shown that dispersion in the presence of a reversible mass-exchange may significantly exceed that obtained for the inert case.

The possibility of inducing mass transfer enhancement using AC-driven EOF has received very little attention in the open literature. Huang and Lai (2006) have presented an analytical study of the enhanced mass transfer in an oscillatory EOF, within a parallel-plate micro-channel configuration. Their results indicated that a modest increase of the mass transfer rate may be accomplished, under the range of parameters investigated. They also illustrated the existence of cross-over phenomena where, under certain conditions, the oscillations induce a larger mass flux for either a slow or fast diffuser.

It is therefore the purpose of this study, to present an analysis of mass transfer in AC-driven EOF, considering an electrically neutral solute undergoing reversible phase exchange with the walls of a capillary tube. The paper is organized as follows: Sect. 2 contains the model derivation and obtained solutions for the velocity and concentration fields, as well as the dispersion coefficient; results are then presented and discussed in Sect. 3, with concluding remarks given in Sect. 4.

2 Model formulation

We consider the velocity field induced by an external electric field, applied along the axis of a cylindrical tube. Axial-symmetry is assumed, eliminating any azimuthal dependence, and we denote r and z as the radial and axial coordinates, respectively. In what follows, the model equations required for obtaining the velocity and concentration fields will be derived, along with the assumptions made. We then present the solutions and the resulting expression for the dispersion coefficient.

2.1 The electric field

In order to find a solution for the EOF problem, the electric field within the tube and, in particular, within the EDL, must first be described. In the forthcoming analysis, it is assumed that the ionic component is a single valence, symmetric solute (e.g., KCl). The distribution of the electric potential is governed by the nonlinear Poisson–Boltzmann equation. However, by invoking the Debye–Hückel approximation, the equation may be linearized, resulting in (Probstein 2003)

$$\frac{1}{\eta}\frac{\mathrm{d}}{\mathrm{d}\eta}\left(\eta\frac{\mathrm{d}\Psi}{\mathrm{d}\eta}\right) = (\chi R)^2\Psi. \tag{1}$$

Here, $\Psi = e_0\psi/kT$ is the scaled potential, with ψ denoting the electric potential, e_0 the elementary charge, k the Boltzmann constant, and T the absolute temperature. We also designate $\eta = r/R$ as the scaled radial coordinate, where R is the tube radius. The parameter χ, defined as

$$\chi = \left(\frac{2e_0^2 n_0}{\epsilon kT}\right)^{1/2}, \tag{2}$$

is the reciprocal of the Debye length, a measure of the characteristic EDL thickness. Here, n_0 denotes the bulk ionic concentration and ϵ is the permittivity of the liquid medium.

The linearized Poisson–Boltzmann equation (1), is subject to the boundary conditions

$$\frac{\mathrm{d}\Psi}{\mathrm{d}\eta} = 0, \quad \eta = 0, \tag{3a}$$

and

$$\Psi = \Psi_\mathrm{s}, \quad \eta = 1, \tag{3b}$$

where Ψ_s is the scaled 'zeta' potential.

The solution to this boundary value problem may be written as

$$\Psi(\eta) = \Psi_s \frac{I_0(\lambda\eta)}{I_0(\lambda)}, \tag{4}$$

in which I_0 is the zeroth order, modified Bessel function of the first kind and $\lambda = \chi R$ is the scaled reciprocal Debye length.

2.2 The velocity field

The equation of motion for an incompressible, fully developed, electrically driven flow in a cylindrical tube is given by:

$$\rho\frac{\partial u}{\partial t} = \frac{\mu}{r}\frac{\partial}{\partial r}\left(r\frac{\partial u}{\partial r}\right) + \rho_e E, \tag{5}$$

where u is the axial velocity component, t is the time, μ, ρ are the fluid's viscosity and density, respectively, and ρ_e is the charge density. The term $\rho_e E$ represents the electric-field body force (Lorentz force), and the pressure gradient is assumed to be negligible compared with the electric body force. The boundary conditions for this equation are no-slip at the solid wall and a finite velocity at the tube axis, i.e.,

$$\frac{\partial u}{\partial r} = 0, \quad r = 0, \tag{6a}$$

and

$$u = 0, \quad r = R. \tag{6b}$$

We consider the velocity distribution under the influence of a uniform, time-harmonic electric field, of the form

$$E(t) = E_0 e^{i\omega t} \tag{7}$$

where E_0 is the amplitude of the applied electric field, i is the imaginary unit, and ω is the angular frequency of the oscillations. Next, we seek the fully periodic solution, after the initial transient has decayed; motivated by the form of the applied electric field, we assume the velocity distribution has the following form:

$$u = \Re[U_\mathrm{s} f(\eta) e^{i\omega t}], \tag{8}$$

in which $\Re[\cdot]$ denotes the real part of a complex quantity. Here, we choose the Helmholz–Smoluchowski velocity $U_\mathrm{s} = \epsilon\psi_\mathrm{s}E_0/\mu$ as the reference velocity, representing the steady-state velocity attainable under a DC electric field of a magnitude E_0.

With these assumptions, and upon substitution of the solution to the linearized Poisson–Boltzmann equation, (5), the equation of motion (6) becomes, in scaled form:

$$i\alpha^2 f - \frac{1}{\eta}\frac{\mathrm{d}}{\mathrm{d}\eta}\left(\eta\frac{\mathrm{df}}{\mathrm{d}\eta}\right) = \lambda^2\frac{I_0(\lambda\eta)}{I_0(\lambda)} \tag{9}$$

subject to the boundary conditions

$$\frac{\mathrm{df}}{\mathrm{d}\eta} = 0, \quad \eta = 0, \tag{10a}$$

and

$$f = 1, \quad \eta = 1. \tag{10b}$$

The solution to this problem may be written as

$$f(\eta) = \frac{i\lambda^2}{\alpha^2 + i\lambda^2}\left(\frac{J_0(\hat{\alpha}\eta)}{J_0(\hat{\alpha})} - \frac{I_0(\lambda\eta)}{I_0(\lambda)}\right), \tag{11}$$

where J_0 is the zeroth order bessel function of the first kind and $\hat{\alpha} = i^{3/2}\alpha$, with α denoting the Womersley number, familiar from pressure-driven oscillating flow. We note that $\alpha^2 = R^2\omega/\nu$ is the ratio of the viscous time scale, R^2/ν to the oscillation time scale, $1/\omega$.

2.3 The concentration field

We now consider the transport of a soluble species, the concentration of which is denoted by C. We assume that this solute is neutral, in the sense that it is not affected by the electric field; rather, its transport is governed by advection through the influence of the electrically driven velocity field, and by diffusion. The solute may undergo a reversible exchange process with the solid wall, and we neglect any possible changes to the charge characteristics and 'zeta' potential of the solid material.

Assuming the surface reaction is described by first-order kinetics, we may write (Ng and Yip 2001; Purnama 1988)

$$\frac{\partial C_\mathrm{s}}{\partial t} = k_\mathrm{a} C - k_\mathrm{d} C_\mathrm{s} \tag{12}$$

where C_s is the adsorbed-phase surface concentration (kg/m^2) and k_a, k_d denote the rate constants for the adsorption and desorption processes, respectively. It then follows that, at equilibrium, the mobile phase and adsorbed phase concentrations are related by

$$C_\mathrm{s} = \sigma C \tag{13}$$

with $\sigma = k_\mathrm{a}/k_\mathrm{d}$ denoting the phase partitioning coefficient, a measure of the affinity which the adsorbate displays toward the adsorbent material. Equation 13 thus describes a linear isotherm.

The concentration field is governed by the following advection–diffusion equation:

$$\frac{\partial C}{\partial t} + u\frac{\partial C}{\partial x} = \frac{D_\mathrm{m}}{r}\frac{\partial}{\partial r}\left(r\frac{\partial C}{\partial r}\right) + D_\mathrm{m}\frac{\partial^2 C}{\partial z^2}, \tag{14}$$

where D_m is the molecular diffusion coefficient. This equation is subjected to the following boundary conditions: a symmetry condition at the tube axis,

$$\frac{\partial c}{\partial r} = 0, \quad r = 0, \tag{15a}$$

and the reversible mass exchange with the tube wall,

$$-D_\mathrm{m}\frac{\partial C}{\partial r} = \frac{\partial C_\mathrm{s}}{\partial t} = k_\mathrm{d}(\sigma C - C_\mathrm{s}), \quad r = R. \tag{15b}$$

Neglecting end effects, we may seek a solution of the form:

$$C(r, z, t) = \gamma\left(z + g(r)e^{i\omega t}\right) \tag{16}$$

and

$$C_\mathrm{s}(z, t) = \gamma\left(z + g_\mathrm{s}(z)e^{i\omega t}\right) \tag{17}$$

where γ is the local axial concentration gradient, which is here assumed to be constant; this form has been used for related problems with a no penetration boundary condition (Chatwin 1975; Watson 1983). However, it may be shown to be a valid assumption for the reactive-wall boundary condition as well (Ng 2006). The function g represents the radial variation of the concentration field, and is the solution to the following boundary value problem, given here in non-dimensional form:

$$i\Omega^2 g - \frac{1}{\eta}\frac{\mathrm{d}}{\mathrm{d}\eta}\left(\eta\frac{\mathrm{d}g}{\mathrm{d}\eta}\right) = -Pef, \tag{18}$$

where f is the scaled radial velocity variation given by Eq. 11, and the following non-dimensional parameters have been defined: the diffusion Péclet number,

$$Pe = \frac{U_\mathrm{s}R}{D_\mathrm{m}} \tag{19}$$

and

$$\Omega^2 = \frac{R^2\omega}{D_\mathrm{m}} = \alpha^2 Sc \tag{20}$$

which is the ratio of the diffusive time scale to the oscillation time scale, and $Sc = \nu/D$ is the Schmidt number. Equation 22 is subject to the boundary conditions

$$\frac{\mathrm{d}g}{\mathrm{d}r} = 0, \quad r = 0, \tag{21a}$$

and

$$-D_\mathrm{m}\frac{\mathrm{d}g}{\mathrm{d}r} = i\omega g_\mathrm{s} = k_\mathrm{d}(\sigma g - g_\mathrm{s}), \quad r = R. \tag{21b}$$

Following Ng (2006), we solve the equality on the right and substitute for g_s, obtaining

$$-D_\mathrm{m}\frac{\mathrm{d}g}{\mathrm{d}r} = \frac{i\omega k_\mathrm{d}\sigma}{k_\mathrm{d} + i\omega}g, \quad r = R, \tag{22}$$

which may be re-cast into the following, dimensionless form:

$$-\frac{\mathrm{d}g}{\mathrm{d}\eta} = \hat{Da}\,g, \quad \eta = 1, \tag{23}$$

in which

$$\hat{Da} = \hat{\beta}Da,$$

where $Da = k_\mathrm{d}R^2/D_\mathrm{m}$ is the Damköhler number, reflecting the ratio of the diffusive time scale and the reaction time scale; we may note that, when $Da \to 0$, or $\sigma \to 0$, this boundary condition reduces to that of an inert solute-wall system.

Here, we have also introduced the definitions

$$\hat{\beta} = \frac{i\omega\tilde{\sigma}}{k_\mathrm{d} + i\omega} = \frac{1 + ik_\mathrm{d}/\omega}{1 + (k_\mathrm{d}/\omega)^2}\tilde{\sigma}, \tag{24}$$

where

$$\tilde{\sigma} = \frac{\sigma}{R}, \quad \frac{k_\mathrm{d}}{\omega} = \frac{Da}{\Omega^2}. \tag{25}$$

Finally, the scaled symmetry condition at the tube axis is

$$\frac{\mathrm{d}g}{\mathrm{d}\eta} = 0, \quad \eta = 0. \tag{26}$$

The function f is given by Eq. 14, and the solution to Eq. 22 is found to be

$$g(\eta) = Pe\left(B_3\frac{J_0(\hat{\Omega}r)}{J_0(\hat{\Omega})} - B_1\frac{I_0(\lambda r)}{I_0(\lambda)} - B_2\frac{J_0(\hat{\alpha}r)}{J_0(\hat{\alpha})}\right) \tag{27}$$

where $\hat{\Omega} = i^{3/2}\Omega$, and the following definitions have been made:

$$B_1 = \frac{\lambda^2}{\left(\lambda^2 - i\alpha^2\right)\left(\lambda^2 - i\Omega^2\right)},$$

$$B_2 = \frac{i\lambda^2}{\left(\lambda^2 - i\alpha^2\right)\left(\alpha^2 - \Omega^2\right)},$$

and

$$B_3 = \frac{B_1(\hat{Da} + G_\lambda) + B_2(\hat{Da} - G_\alpha)}{\hat{Da} - G_\Omega},$$

in which

$$G_\lambda = \lambda\frac{J_1(\lambda)}{J_0(\lambda)}, \quad G_\alpha = \hat{\alpha}\frac{J_1(\hat{\alpha})}{J_0(\hat{\alpha})}, \quad G_\Omega = \hat{\Omega}\frac{J_1(\hat{\Omega})}{J_0(\hat{\Omega})}.$$

2.4 The time-averaged mass flux

Having found the solutions describing the velocity and concentration distributions, we now turn to evaluate the mass flux.

Using a multiple time-scale homogenization technique, Ng (2006) has shown that the 'effective diffusion', or

dispersion coefficient, resulting from the oscillating velocity and concentration fields, may be expressed as

$$D_{\mathrm{e}} = -\frac{1}{2\mathcal{R}_d}\Re[\langle u^* g\rangle] \tag{28}$$

where the star denotes a complex conjugate, angle brackets represent a cross-sectional average and $\mathcal{R}_d = 1 + 2\tilde{\sigma}$ is a retardation factor, appearing as a consequence of the solute partitioning between the mobile and adsorbed phases. Additionally, there will be a mass flux due to ordinary molecular diffusion, $\mathbf{j}_D = AD_{\mathrm{m}}\gamma$. It is convenient to express the mass flux as the ratio of the convective contribution to that of molecular diffusion, enabling a direct assessment of any substantial increase in the mass flux due to the flow oscillations. Thus, we may write

$$\frac{D_{\mathrm{e}}}{D_{\mathrm{m}}} = 1 - \frac{Pe}{2\mathcal{R}_d}\Re[\langle f^* g\rangle], \tag{29}$$

which differs from the form found by Watson (1983) and Kurzweg (1985) by the presence of the retardation factor.

In order to illustrate the frequency dependence of the dispersion coefficient, it is convenient to employ the concept of a tidal displacement, which may be described as the average axial distance traversed by a fluid particle during half an oscillation cycle. As such, it is a useful measure of the oscillation amplitude. We therefore introduce the tidal displacement as

$$\Delta z = \frac{U_{\mathrm{s}}\langle f\rangle}{\omega} = 2U_{\mathrm{s}}\left|\int_0^{\frac{\pi}{\omega}} e^{i\omega t}\mathrm{d}t \int_0^1 \eta f(\eta)\mathrm{d}\eta\right|. \tag{30}$$

Performing the integration yields

$$\Delta z = \frac{2}{\omega}\frac{\lambda^2}{\alpha^2 + i\lambda^2}(F_\lambda + F_\alpha). \tag{31}$$

Next, we re-express the Péclet number using the tidal displacement, as follows

$$Pe = \frac{U_{\mathrm{s}}R}{D} = \frac{\omega\Delta z R}{|\langle f\rangle|D} = \frac{\Omega^2}{|\langle f\rangle|}\Delta Z, \tag{32}$$

with $\Delta Z = \Delta z/R$; this, in effect, defines a frequency-dependent Péclet number.

Finally, substituting the expressions for the functions f and g and performing the required integration, we find

$$\begin{aligned} D_{\mathrm{e}} = Pe\Re\Bigg[&\frac{\lambda^2}{\lambda^2 + i\alpha^2}\Bigg(B_1\left(G - \frac{G_\lambda + G_\alpha^*}{\lambda^2 + i\alpha^2}\right) \\ &+ B_2\left(\frac{2i\alpha^2 G_\lambda - (\lambda^2 - i\alpha^2)G_\alpha^* + (\lambda^2 + i\alpha^2)G_\alpha}{2i\alpha^2(\lambda^2 - i\alpha^2)}\right) \\ &- B_3\left(\frac{i\alpha^2(1+Sc)G_\lambda - (\lambda^2 - i\Omega^2)G_\alpha^* + (\lambda^2 + i\alpha^2)G_\Omega}{i\alpha^2(\lambda^2 - i\Omega^2)(1+Sc)}\right)\Bigg)\Bigg] \end{aligned} \tag{33}$$

where

$$G = \frac{1}{2}\left(1 - \frac{I_1^2(\lambda)}{I_0^2(\lambda)}\right)$$

3 Results and discussion

In what follows, we present the calculated distributions of the velocity and concentration fields, as well as the dispersion coefficient. These will be illustrated in terms of the pertinent dimensionless variables: λ, characterizing the EDL thickness; α, representing the combined effect of the system geometry and oscillation frequency; Sc, a measure of the solution transport properties, and Da, signifying the relative importance of the adsorption kinetics. The scaled tidal displacement, ΔZ, will be used as a measure of the oscillation amplitude.

Unlike pressure-driven oscillatory flow, there are certain constraints on the magnitude of the frequency and forcing when applying an electric field to drive the oscillations. In terms of the frequency, EOF's enable a relatively wide range of frequencies, which are readily attainable; however, it is generally accepted that these must be kept below ~ 1 MHz, if EDL relaxation effects are to be avoided. While this places an upper limit on the possible range of values used for α, this constraint is easily adhered to for the range of values used herein, as the following numerical example illustrates: in an aqueous solution with $\nu \approx 10^{-6}\,\mathrm{m}^2/\mathrm{s}$, a value of $\alpha = 0.5$ corresponds with a frequency of ~ 4 Hz in a tube with $R = 100$ μm, while for a pore with $R = 1$ μm, a frequency of 1600 Hz corresponds with a value of $\alpha \approx 0.1$. The constraint on the applied electric field amplitude restricts the magnitude of the forcing applied to generate the oscillations, so as to avoid Joule heating and possible electro-kinetic instabilities; it has been suggested that $E_0 < 100$ V/mm is an acceptable limit on the applied electric field (Huang and Lai 2006). In terms of the scaled tidal displacement, $\Delta Z = 1$ is readily achievable with $\alpha = 0.5$ in a tube with $R = 100$ μm, while for a tube with $R = 1$ μm, $\alpha = 0.1$ easily conforms with these restrictions. For smaller radii, it becomes increasingly difficult to adhere to these constraints, while keeping $\Delta Z > 1$; however, it is unclear whether instabilities may occur at such small scales. It may also be noted that Joule heating may not necessarily be detrimental to the processes under consideration; nevertheless, as the presented analysis does not account for these effects, these assumptions must be justifiable.

We now turn to illustrate the characteristics of the flow and concentration fields, as well as the resulting effect on the solute mass transfer. The velocity distribution at

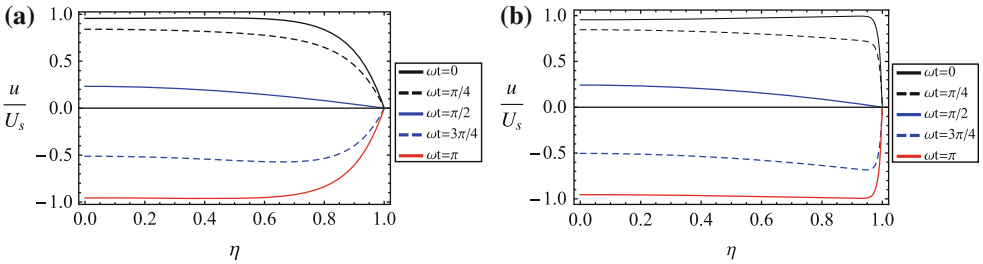

Fig. 1 Scaled velocity distribution, at different times during an oscillation cycle. **a** $\alpha = 1$, $\lambda = 10$. **b** $\alpha = 1$, $\lambda = 100$

different times during an oscillation cycle, is shown in Fig. 1, calculated with $\alpha = 1$, illustrative of the range employed in this study. Also shown is the effect of the EDL thickness, manifested through the parameter λ. For $\alpha = 1$, the velocity evolves toward a "plug flow" profile, characteristic of DC-driven EOF. The maximum velocity attainable during an oscillation cycle is equal to that of a fully developed DC-driven EOF. This is also expected for values of $\alpha < 1$; at this range of values, the viscous time scale is comparable with or smaller than the oscillation time scale, and so momentum transfer affects the whole cross-section during an oscillation period. As α is increased, the velocity distribution deviates from this behavior, most of the flow being driven in or close to the EDL and the fluid at the center of the tube lags behind; at sufficiently high values of α, the flow oscillations become confined to a boundary layer region and the fluid far from the wall is not affected by the motion. The maximum velocity reached during a cycle is accordingly smaller (not shown). A thinner EDL results in a sharp decrease of the velocity near the wall, where a no-slip condition is imposed; when the EDL is thicker, a greater part of the tube is influenced by the electric field and the velocity declines to zero more gradually. The scaled radial concentration field, represented by the function g, is shown in Fig. 2, for $\alpha = 1$; it may be seen that the radial concentration distribution is nearly uniform, except for the wall regions where a gradient develops. The retentive boundary alters the concentration distribution to various degrees, strongly dependent upon the adsorption kinetics, as illustrated in Fig. 3. The concentration at the retentive wall is always higher than that found for the inert case. As some of the solute is adsorbed onto the surface, transport occurs due to this interaction and not solely through diffusion induced by the velocity non-uniformity; this effect is further enhanced as the desorption kinetics become faster since, under such conditions, the adsorbed solute is readily exchanged with the mobile phase.

Next, we examine the mass transfer resulting from the presence of the oscillating concentration and velocity fields. The effect of α on the degree of enhancement, shown in terms of the ratio D_e/D_m, is plotted in Fig. 4, for values of the Schmidt number ranging between 1000 and 5000, corresponding with molecular diffusivities of 10^{-9}–2×10^{-10} m^2/s, respectively (note that, in general, the potential enhancement increases for slower diffusers). The calculated dispersion coefficient generally exhibits characteristics found in related studies of dispersion in

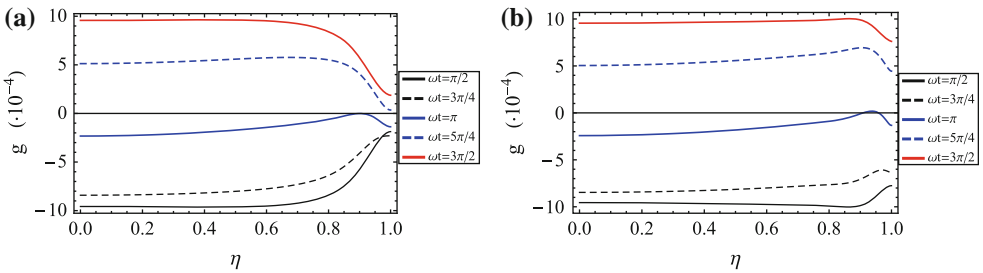

Fig. 2 The function g, representing the scaled radial concentration distribution, at different times during an oscillation cycle. **a** $\alpha = 1$, $\lambda = 10$. **b** $\alpha = 1$, $\lambda = 100$. Calculations made with $Da = 1$, $\sigma = 1$, $Pe = 1$, and $Sc = 1000$

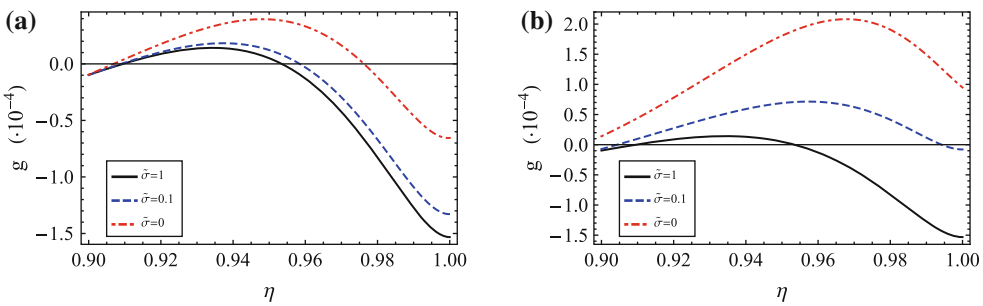

Fig. 3 Effect of boundary retention on the scaled concentration distribution. **a** Intermediate kinetics, $Da = 1$. **b** Fast kinetics, $Da = 10$. Calculations were made for $\alpha = 1$, $\omega t = \pi$, $Sc = 1000$, and $\lambda = 100$

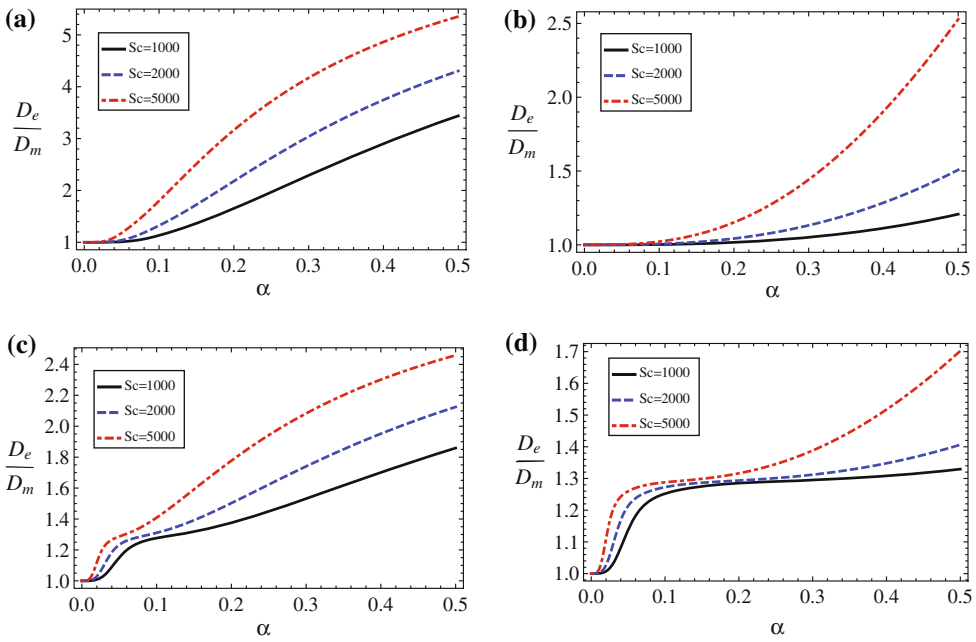

Fig. 4 The variation of the mass transfer enhancement, represented by the ratio D_e/D_m, with the Womersley number α, for various values of the Schmidt number, Sc. **a** $\tilde{\sigma} = 0,\ \lambda = 10$. **b** $\tilde{\sigma} = 0,\ \lambda = 100$. **c** $\tilde{\sigma} = 1,\ \lambda = 10$. **d** $\tilde{\sigma} = 1,\ \lambda = 100$. All calculations were made for $\Delta Z = 1$ and $Da = 1$

oscillatory flows (e.g., Watson 1983); the dispersion coefficient increases with α and is shown to favor the slower diffusers. However, the curves are shifted towards lower values of α, through both the effect of the EDL thickness and boundary retention. A thicker EDL results in a larger dispersion coefficient, due to stronger concentration gradients. Under the values of α considered, the velocity distribution outside the EDL is uniform, and so the velocity non-uniformity exists solely within the EDL; consequently, a thicker EDL allows for a larger zone over which velocity variations create concentration gradients. Moreover, for a constant tidal displacement, a larger forcing is required in the case of a thick EDL, since the maximum attainable velocity is lower than the corresponding thin EDL case.

As already mentioned, the mass transfer process manifested through the dispersion coefficient, relies on solute diffusion into and out of the slower moving regions of the velocity field—we shall refer to this mode of transport as 'shear induced'. This type of temporal 'storage', in the presence of an axial concentration gradient, results in a time-averaged flux which can be described naively as a ratchet like motion of the solute. The process relies on appropriate temporal phasing between diffusion and axial advection; for example, a slow diffusing substance will, in general, require low frequencies in order to diffuse into and out of the viscous boundary during half an oscillation cycle. When adsorption and desorption occur at the wall, an additional 'storage' mechanism is present. This adds complexity to the process, as now there is an interplay between the amount of solute potentially adsorbed, determined by the partition factor, σ, and its ability to be released back into the mobile phase, controlled by the desorption rate constant, k_d; furthermore, diffusion to and from the wall may still remain an important factor. As an illustration of this intricate behavior, Fig. 5 shows the variation of the dispersion coefficient as a function of the scaled partition factor, $\tilde{\sigma}$, with different adsorption kinetics, manifested through the Damköhler number, Da. It may be seen that, for most cases, an increase of the dispersion coefficient is predicted when wall retention comes into play. Several interesting features may be pointed out, the most striking of which is the existence of a clear maximum in the degree of enhancement achievable through boundary mass exchange; this maximum shifts according to the frequency, and may indeed be traced to the frequency dependent parameter $\hat{Da}$, introduced in the scaled boundary condition given by Eq. 23. This parameter reflects the frequency response of the boundary reaction, and includes the terms k_d/ω, the ratio of the desorption rate and the angular frequency. This characteristic of the dispersion coefficient was previously presented by Ng (2006), who showed that the greatest effect is observed for slow kinetics ($Da = 0.1$); in the present calculations, this maximum is most prominent for fast kinetics ($Da = 10$), which seems to be in contradiction. However, it turns out that the transport characteristics of the solution come into play here, as Ng (2006) made the calculations for $Sc = 0.1$ while we present calculations for $Sc = 1000$, where diffusion is several orders of magnitude slower. Curiously, for an intermediate case ($Sc = 10$), the maximum has the greatest value for $Da = 1$, i.e., when reaction kinetics are comparable with diffusion (not shown). The occurrence of this maximum may be attributed to the fact that boundary retention allows for a greater temporal 'storage' which,

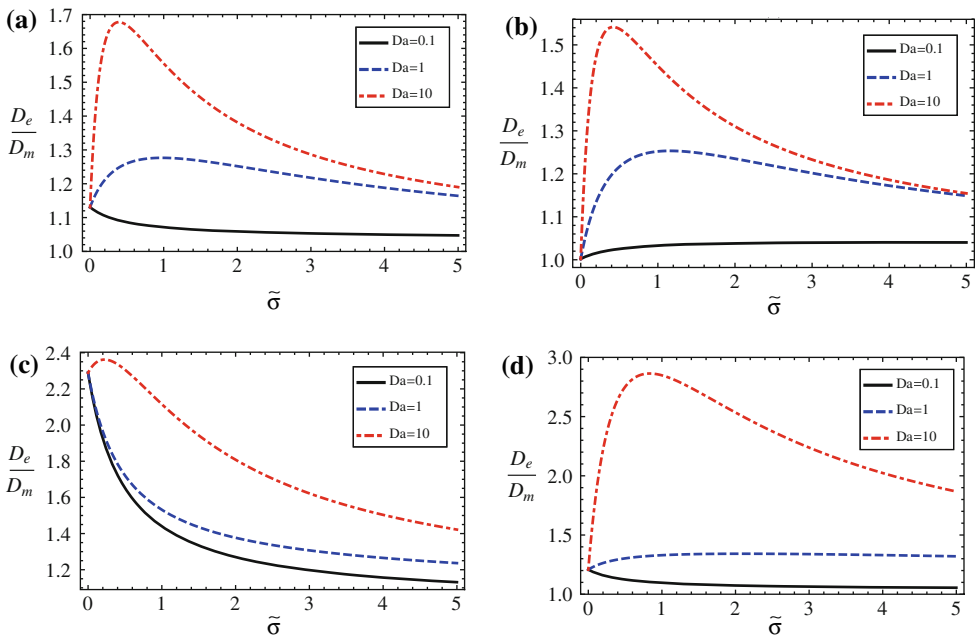

Fig. 5 Effect of the solute partitioning factor, $\tilde{\sigma}$, on the mass transfer enhancement, represented by the ratio D_e/D_m. **a** $\alpha = 0.1$, $\lambda = 10$. **b** $\alpha = 0.1$, $\lambda = 100$. **c** $\alpha = 0.5$, $\lambda = 10$. **d** $\alpha = 0.5$, $\lambda = 100$. All calculations were made with $\Delta Z = 1$ and $Sc = 1000$

under appropriate flow conditions, enhances the mass transfer. However, as the partitioning is increased, the retardation factor weighs down the ability of the solute to be 'shuttled' along the concentration gradient, and the dispersion coefficient decreases. In fact, when the kinetics are slow, the dispersion process is more akin to the inert boundary case, and the solute partitioning has the sole effect of retarding the transport of the reactive solute.

Another noteworthy feature is the effect of the EDL thickness. When a thick EDL is present, the calculations made with $\alpha = 0.5$ illustrate that the adsorption process reduces the dispersion coefficient, regardless of kinetics, while in the presence of a thin EDL adsorption still exhibits a maximum for fast and intermediate kinetics. This may be attributed to the fact that when the EDL is thin, the shear-mediated diffusive contribution to the dispersion is greatly reduced. Note that the intercept at $\tilde{\sigma} = 0$ signifies the degree of enhancement obtained for an inert solute-wall system; for $\alpha = 0.1$, this value is 1.13 when $\lambda = 10$, while it is merely 1.002 when $\lambda = 100$, indicating that under these conditions, no enhancement is expected in the inert system, in agreement with the results shown by Huang and Lai (2006). This may be expected as the plug flow, characteristic of thin EDL's, does not promote shear-induced dispersion. In such a case, solute exchange with the wall is the sole contribution to the mass transfer enhancement.

Thus far, we have examined some of the characteristics of the dispersion coefficient, and particularly the intricate interplay between the properties of the EDL and resulting flow field with the solution transport properties and the solute-wall interaction parameters. However, the practical implication emerging from this analysis is the possibility of separating solute species in an oscillatory EOF, mediated by the degree of boundary interaction. This has previously been explored for pressure-driven oscillatory flow in a tube with an absorbing 'gel' coating the inner wall (van Lishout and Leighton 1996), while other studies have considered separation based on shear-induced dispersion of solutes with different diffusivities (Jaeger 1985). First, we note that the results shown in Fig. 5 suggest that such a separation may be achieved through a difference in adsorption kinetics. For example, with $\lambda = 100$, $\alpha = 0.5$, and $\tilde{\sigma} \simeq 0.8$, the transport of a solute with fast kinetics ($Da = 10$) may be increased threefold compared to a solute with slow kinetics ($Da = 0.1$). Note that this is calculated for a scaled tidal displacement of $\Delta Z = 1$; in a capillary with $R = 100$ μm, $\alpha = 0.5$ corresponds with a frequency of 4 Hz and so a value of $\Delta Z = 10$ should still be well within the constraints imposed on the magnitude of the applied forcing. Under such conditions, the enhancement is calculated to be nearly 185-fold for fast kinetics, compared with 11.4 for slow kinetics, or a ratio of $\simeq 16$.

Another, perhaps more obvious attribute which is commonly exploited, is the degree of affinity a solute exhibits towards the adsorbing material. Figure 6 compares the dispersion coefficients calculated for solutes with a varying partition factor, as a function of α and, again, with different EDL thicknesses and kinetics. When $\lambda = 10$, $\alpha = 0.5$, and $Da = 0.1$, the inert solute is favored, its rate of mass transfer reaching nearly twice as much as a solute with $\tilde{\sigma} = 1$. On the other hand, when $\lambda = 100$ and $Da = 10$, the mass flux of a solute with $\tilde{\sigma} = 1$ is nearly two and a half times as much as that of an inert solute. Under identical conditions, increasing the forcing to $\Delta Z = 10$ will result in a ratio of $\simeq 8.5$ for the

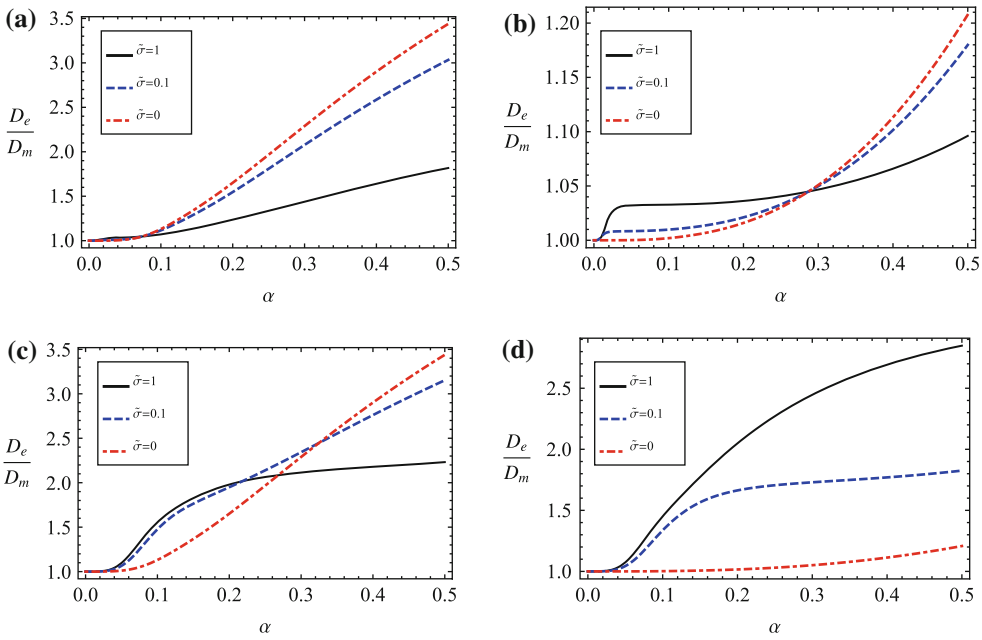

Fig. 6 The variation of the mass transfer enhancement, represented by the ratio D_e/D_m, with the Womersley number α, for various values of $\tilde{\sigma}$. **a** $Da = 0.1$, $\lambda = 10$. **b** $Da = 0.1$, $\lambda = 100$. **c** $Da = 10$, $\lambda = 10$). **d** $Da = 10$, $\lambda = 100$. All calculations were made for $\Delta Z = 1$ and $Sc = 1000$

dispersion coefficients. Intermediate cases show no clear-cut advantage and exhibit complex, frequency dependent, cross-over phenomena, where either an inert or reactive solute is favored. According to the above estimates, kinetic based separation seems to offer a slightly better potential than affinity based separation. This is due to the fact that the inert boundary condition may be recovered in the limit of very slow kinetics ($Da \ll 1$); when the boundary mass exchange is very slow, its combination with the retardation factor reduces the dispersion to values below those of the inert case. However, it is the EDL thickness, an attribute intrinsic to EOF's, which plays a crucial role in the potential separation. As illustrated in Fig. 7, for a thin EDL, mass transfer enhancement may not be achieved for a solute exhibiting slow adsorption kinetics, as well as an inert solute; conversely, the reactive solute with fast kinetics will benefit from a thin EDL. This is a particular characteristic of EOF, where it appears that the shear-mediated time-averaged mass flux may be eliminated. The mechanism which then becomes dominant is a mass exchange between the oscillating fluid core and the wall.

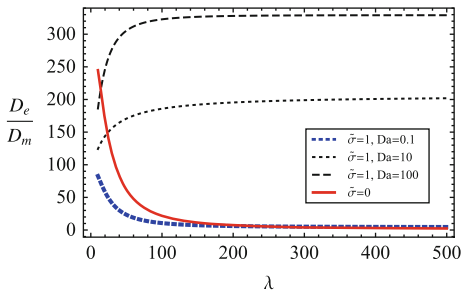

Fig. 7 The variation of the mass transfer enhancement, represented by the ratio D_e/D_m, with λ, for various combinations of $\tilde{\sigma}$ and Da. All calculations were made for $\Delta Z = 10$, $\alpha = 0.5$, and $Sc = 1000$

These results suggest that when the fluid-wall mass exchange approaches equilibrium, the mass transfer may be significantly enhanced for a thin EDL, at a given value of α; moreover, under such conditions this enhancement may be selectively applied to the reactive solute, facilitating a potentially effective separation mechanism. While a DC-driven component may be superimposed on the oscillating EOF, the described separation mechanism may find particular application where such a throughput is unwanted, such as a selective extraction of a single or multiple component from a mixture without imposing a net mass flux of the entire mixture.

It should be noted that, in the presented model, possible variations of the surface charge as a result of the adsorption process are not accounted for. This may not be a good approximation for charged macromolecules such as proteins; alteration of the surface charge will effect the EDL and therefore the flow field, and hence will have an impact on the dispersion process (Ghosal 2002, 2003). However, a charged solute will not be neutral with respect to the applied electric field and so these cases are beyond the scope of the presented analysis.

4 Summary and conclusions

In the presented paper, the mass transfer characteristics of oscillatory EOF in a cylindrical tube were theoretically studied, including the effect of a reversible mass exchange at the solid boundary. In particular, an expression for the

time averaged mass flux, or dispersion coefficient, was obtained analytically.

Under the influence of the reversible wall mass exchange, the dispersion coefficient exhibits a complex dependence on the various parameters representing the effects of the EDL thickness, oscillation frequency, solution transport properties, solute partitioning, and reaction kinetics. In a given geometry, the dispersion increases with the frequency at a constant tidal displacement, as is generally observed for dispersion in oscillating flows. Solute wall exchange may enhance the dispersion, up to a point where the retardation effect, caused by the solute partitioning, becomes sufficiently large so as to delay the transport of the solute down the concentration gradient. The effect of the EDL thickness has been found to be of particular importance in determining the degree of mass transfer enhancement. In the presence of a thick EDL, dispersion is induced both by temporal 'storage' due to diffusion into the slow moving wall region, as well as by exchange with the wall; however, for a thin EDL with $\alpha \leq 1$, the diffusive mode of dispersion is all but eliminated, since the flow becomes nearly uniform and does not induce significant transverse concentration gradients. Under such conditions, wall exchange becomes the dominant mechanism for the time-averaged mass flux. This seems to be a unique feature of the EOF, and is not possible in a pressure-driven flow. Moreover, under such conditions, and for the high Schmidt number solutions considered, fast kinetics increase the mass transfer; in fact, the highest degree of enhancement may be achieved when the wall exchange is governed by the equilibrium relation, i.e., diffusive transport is not a limiting factor.

Our results suggest that an oscillatory EOF with reversible wall exchange may be used for separation of species. This separation may be kinetic-based or affinity-based, with a slight advantage for kinetic-based separation under certain conditions. The sharpest potential separation is achieved under plug-flow conditions, where an inert solute, or one with slow exchange kinetics, experiences virtually no dispersion, while the dispersion is maximized for the reactive solute exhibiting fast kinetics. Such a mode of separation may find interesting application in cases where a component is to be extracted from a mixture without imposing any net bulk motion.

References

Aris R (1960) On the dispersion of a solute in pulsating flow trough a tube. Proc R Soc A 259:370–376

Bhattacharya A, Masliah JH, Yang J (2003) Oscillating laminar electrokinetic flow in infinitely extended circular microchannels. J Colloid Interface Sci 261:12–20

Chang C, Yang R (2007) Electrokinetic mixing in microfluidic systems. Microfluid Nanofluid 3(5):501–525

Chatwin PC (1975) On the longitudinal dispersion of passive contaminant in oscillating flow in tubes. J Fluid Mech 71: 513–527

Dutta P, Beskok A (2001) Analytical solution of time periodic electroosmotic flows: analogies to Stokes' second problem. Anal Chem 73(21):5097–5102

Erickson D, Li D (2003) Analysis of alternating current electroosmotic flows in a rectangular microchannel. Langmuir 19(13): 5421–5430

Ghosal S (2002) Effect of analyte adsorption on the electroosmotic flow in microfluidic channels. Anal Chem 74(4):771–775

Ghosal S (2003) The effect of wall interactions in capillary-zone electrophoresis. J Fluid Mech 491:285–300

Huang HF, Lai CL (2006) Enhancement of mass transport and separation of species by oscillatory electroosmotic flows. Proc R Soc A 462:2017–2038

Jaeger MJ (1985) Diffusion and dispersion in steady counterflow: a method for the separation of gases using enhanced mass transport in oscillatory flow. Chem Eng Sci 53(20):3613–3621

Joshi CH, Kamm RD, Drazen JM, Slutsky AS (1983) An experimental study of gas exchange in laminar oscillatory flow. J Fluid Mech 133:245–254

Kang Y, Yang C, Huang X (2002) Dynamic aspects of electroosmotic flow in a cylindrical microcapillary. Int J Eng Sci 40(20): 2203–2221

Kurzweg UH, Howell G, Jaeger MJ (1984) Enhanced dispersion in oscillatory flows. Phys Fluids 27(5):1046–1048

Kurzweg UH (1985) Enhanced heat conduction in oscillating viscous flows within parallel-plate channels. J Fluid Mech 156:291–300

Ng CO (2006) Dispersion in steady and oscillatory flows through a tube with reversible and irreversible wall reactions. Proc R Soc A 462:481–515

Ng CO, Yip TL (2001) Effects of kinetic sorptive exchange on solute transport in open-channel flow. J Fluid Mech 446:321–345

Probstein RF (2003) Physicochemical hydrodynamics: an introduction, 2nd edn. New York: Wiley

Purnama A (1988) Boundary retention effects upon contaminant dispersion effects in parallel flows. J Fluid Mech 195:393–412

Squires TM, Quake SR (2005) Microfluidics: fluid physics at the nanoliter scale. Rev Mod Phys 77(3):977–1026

Stone HA, Stroock AD, Ajdari A (2004) Engineering flows in small devices: microfluidics toward a lab-on-a-chip. Annu Rev Fluid Mech 36:381–411

van Lishout YMM, Leighton DT (1996) Absorption-induced separations in oscillatory liquid chromatography. AIChE J 42(4): 940–952

Watson EJ (1983) Diffusion in oscillatory pipe flow. J Fluid Mech 133:233–244

Yang C, Ng CB, Chan V (2002) Transient analysis of electroosmotic flow in a slit microchannel. J Colloid Interface Sci 248(2): 524–527